

Supporting information:

Understanding nitrate formation in a world with less sulfate.

1

Petros Vasilakos¹, Armistead Russell², Rodney Weber³, and Athanasios Nenes^{1,3,4,5†}

¹ School of Chemical and Biomolecular Engineering, Georgia Institute of Technology, Atlanta, Georgia, 30332, USA

² School of Civil and Environmental Engineering, Georgia Institute of Technology, Atlanta, Georgia, 30332, USA

³ School of Earth and Atmospheric Sciences, Georgia Institute of Technology, Atlanta, Georgia, 30332, USA

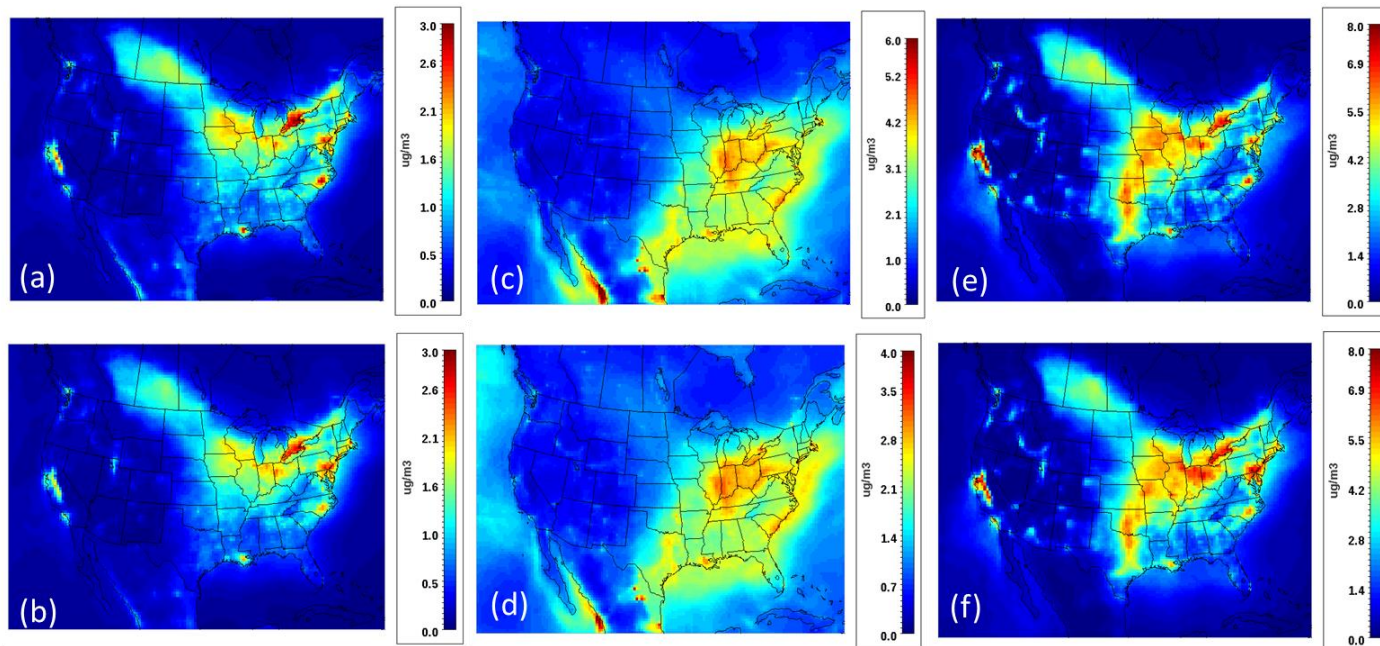
⁴ Institute of Chemical Engineering Sciences, Foundation for Research and Technology-Hellas, Patras, GR 26504, Greece

⁵ Institute for Environmental Research and Sustainable Development, National Observatory of Athens, Palea Penteli, GR 15236, Greece

†Corresponding Author: A. Nenes (athanasios.nenes@gatech.edu)

2

3



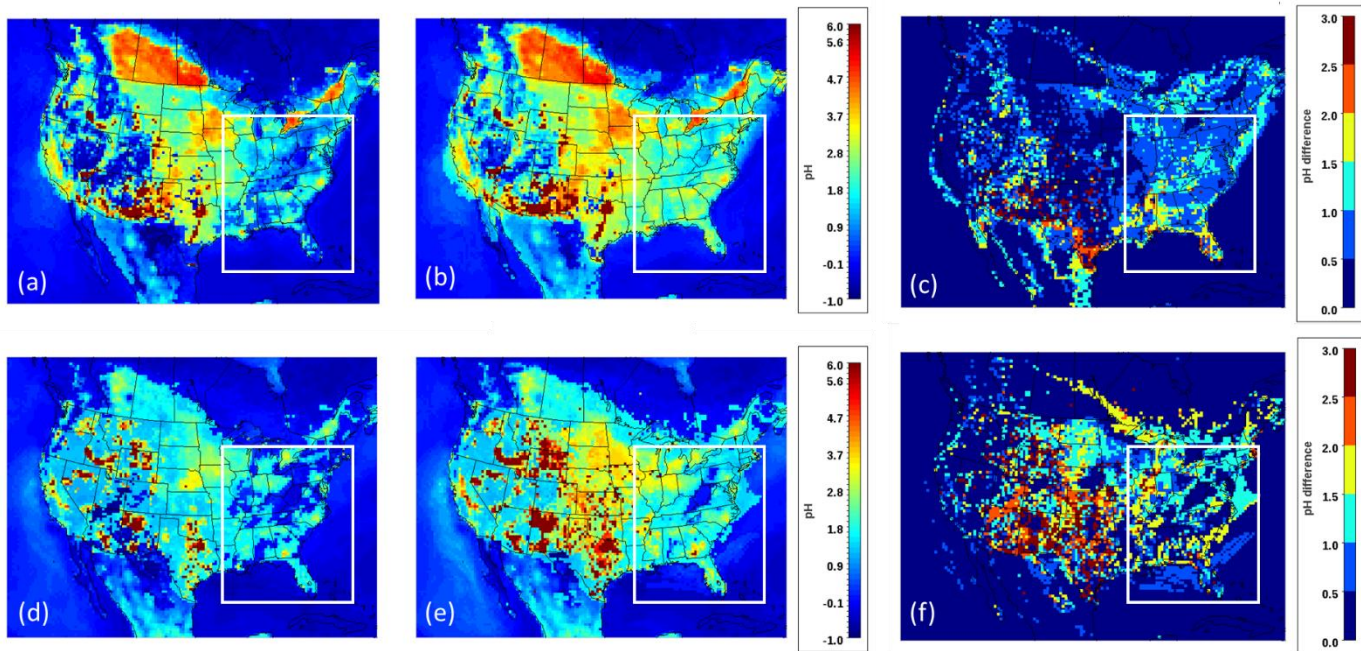
4
 5 **Figure S1** - Yearly averaged predicted concentration fields of (a) 2001 NH₄, (b) 2011 NH₄, (c)
 6 2001 SO₄ (d) 2011 SO₄, (e) 2001 NO₃, (f) 2011 NO₃. Color scales between years are kept the same
 7 for parity, except for sulfate, due to its drastic reduction during the decade

8
 9 **Table S1** – Yearly domain averages and standard deviations for ammonium, sulfate and nitrate
 10 in $\mu\text{g m}^{-3}$ for 2001 & 2011

2001	<i>NH₄</i>	<i>SO₄</i>	<i>NO₃</i>	2011	<i>NH₄</i>	<i>SO₄</i>	<i>NO₃</i>
Domain average	0.42	1.67	1.28	Domain average	0.40	1.20	1.27
St.dev	0.47	1.02	1.43	St.dev	0.45	0.63	1.48

11

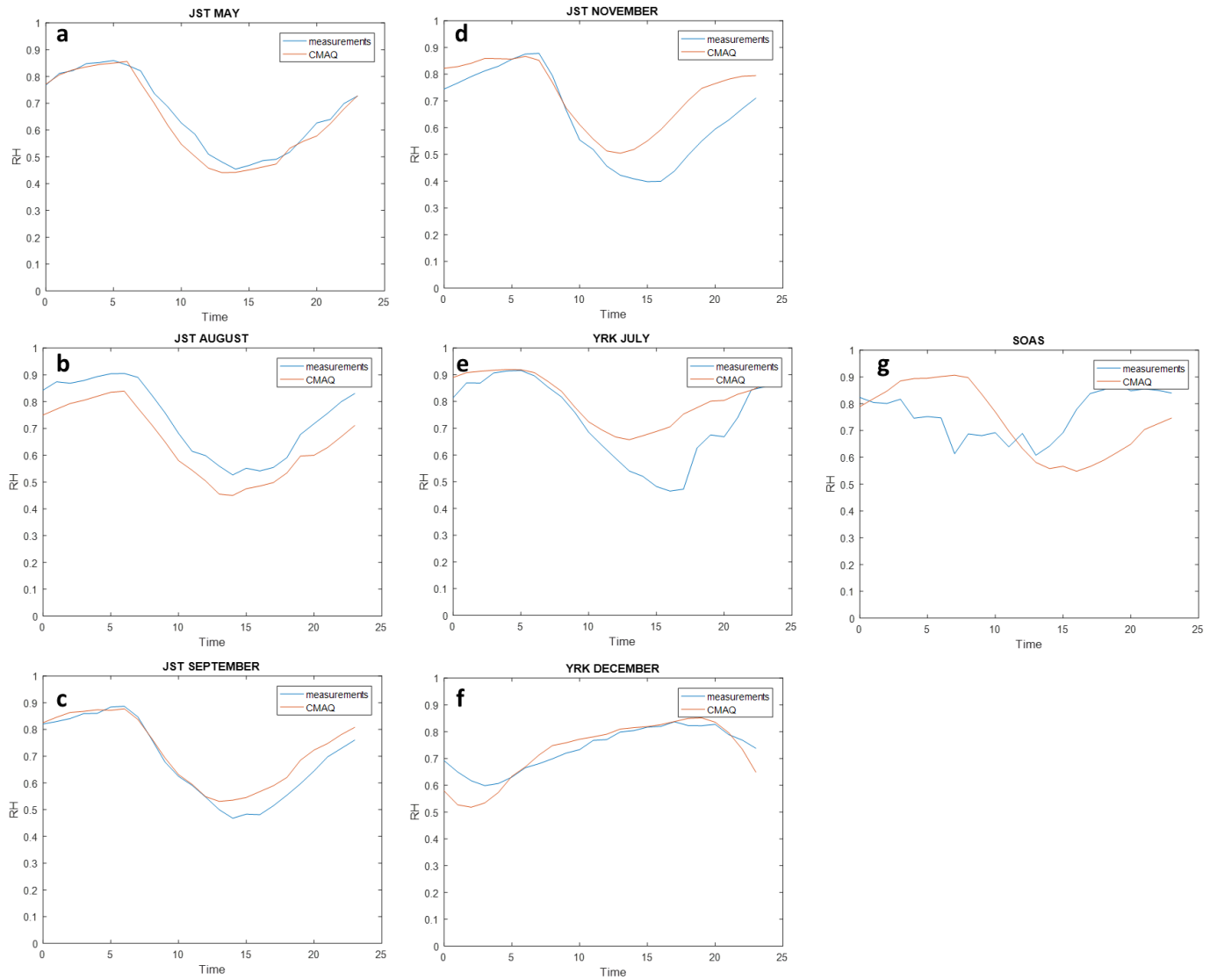
12



13

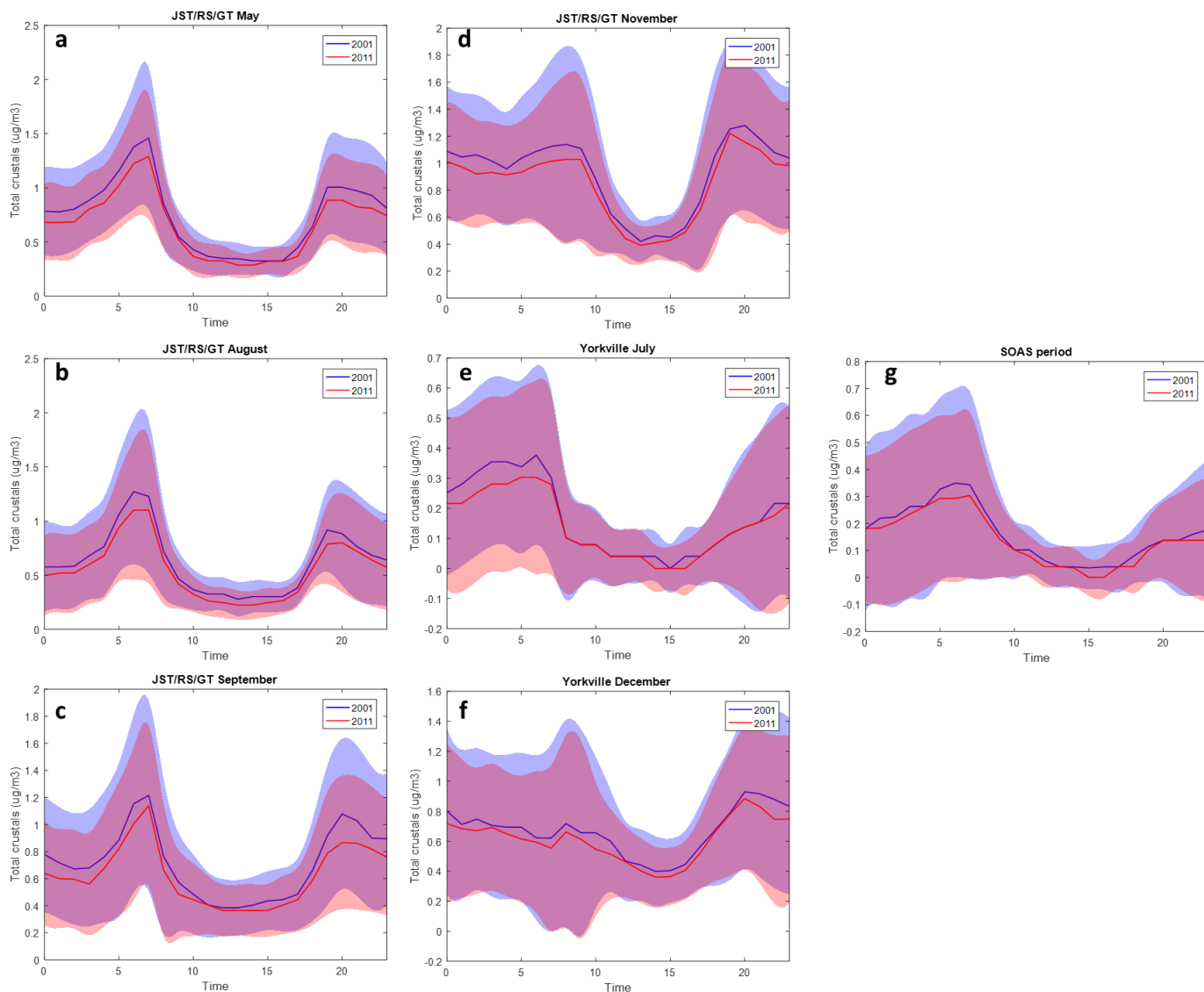
14 **Figure S2** - Seasonally averaged pH over CONUS for the winter (January) of (a) 2001, (b) 2011,
 15 the summer (July) of (d) 2001, (e) 2011. Panel (c) is difference between the simulation years for
 16 the winter, and (f) is the difference for the summer. As in Figure 3, the study domain is highlighted.

17



18
 19 **Figure S3** – RH diurnal profiles for May (a), August (b), September (c) and November (d) at
 20 JST/RS/GT, July (e) and December (f) at YRK and for the SOAS campaign period (g). Blue line
 21 is the CMAQ predicted RH for 2001 and 2011, while the red line represents the measurements

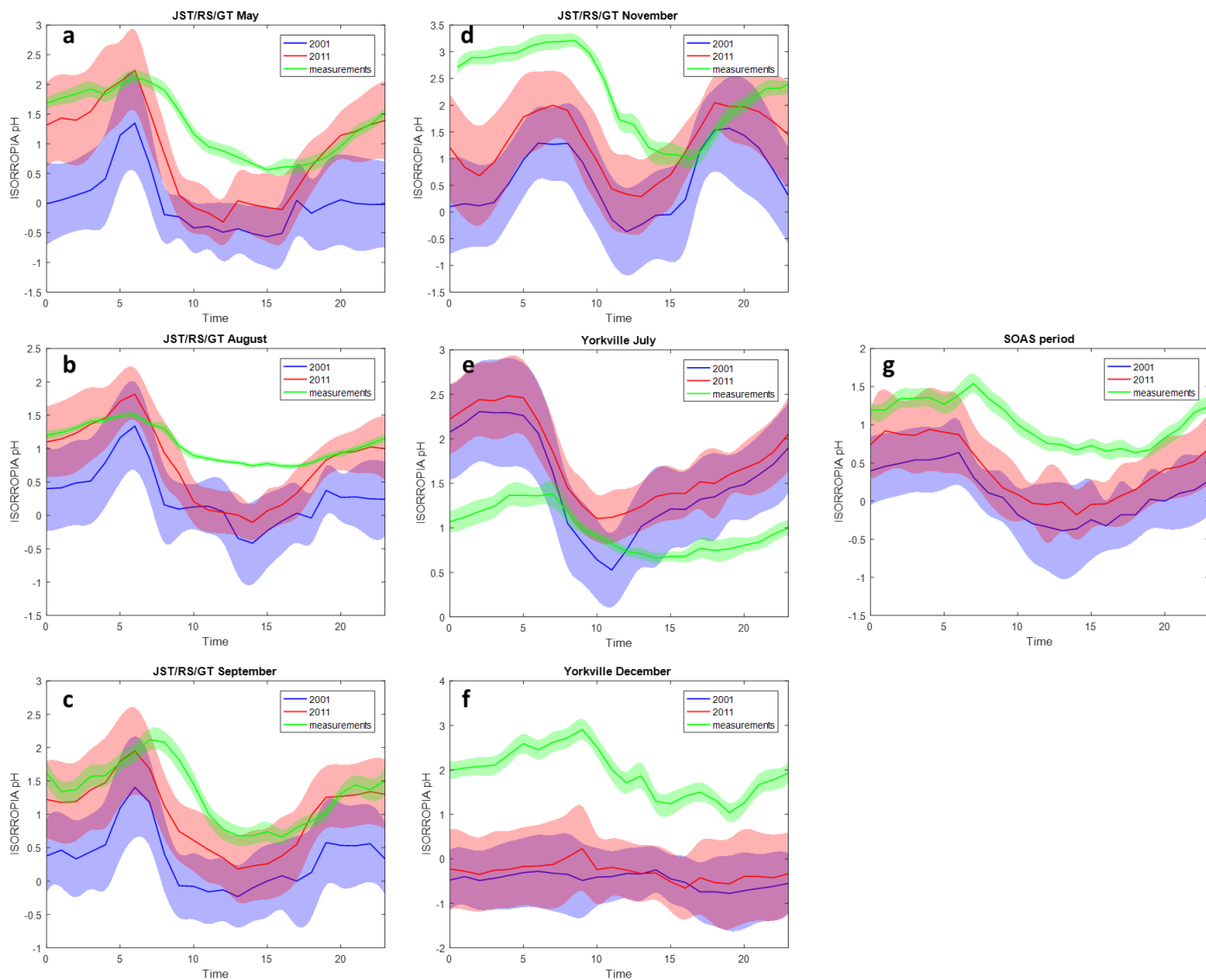
22



23

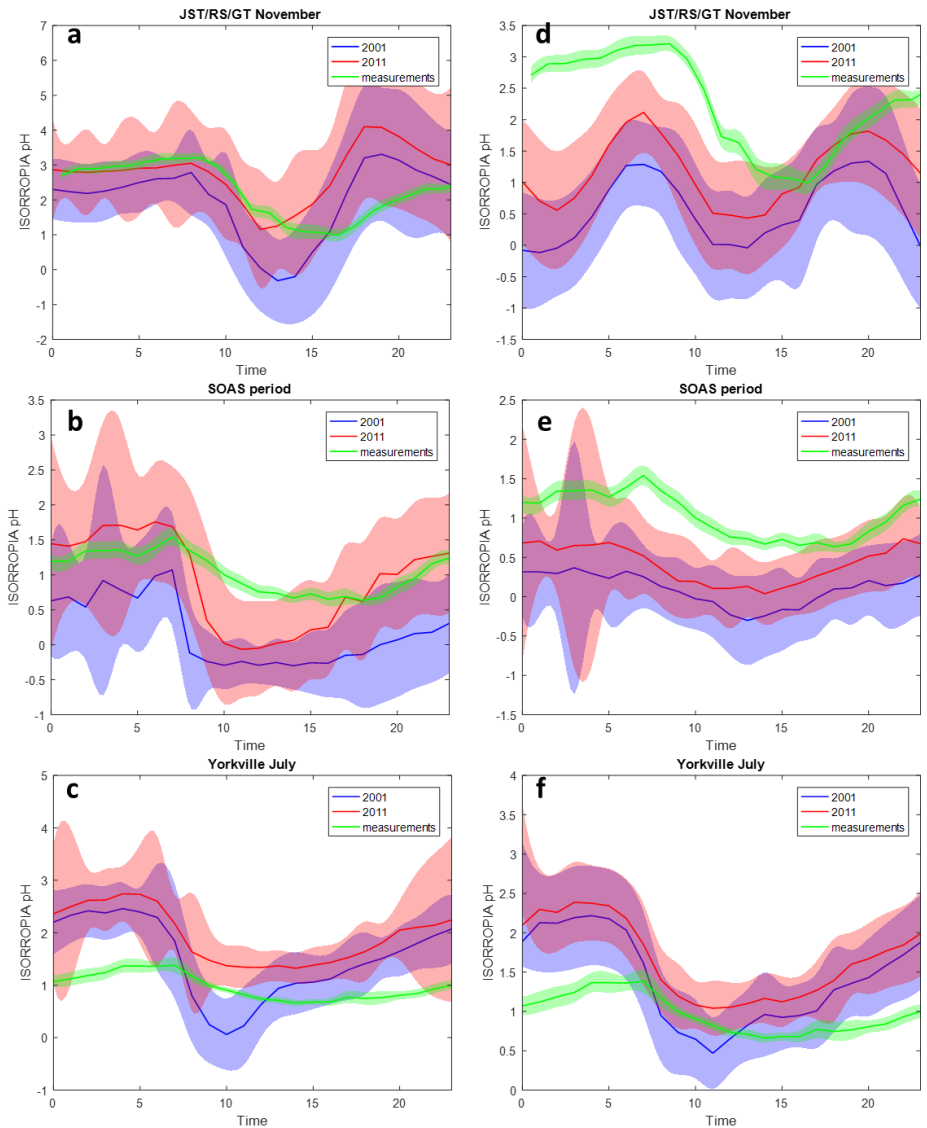
24 **Figure S4** – Total NVC diurnal profiles (Na^+ , Ca^{+2} , K^+ and Mg^{+2}) for May (a), August (b),
 25 September (c) and November (d) at JST/RS/GT, July (e) and December (f) at YRK and for the
 26 SOAS campaign period (g). Blue and red lines are the CMAQ predicted NVCs for 2001 and 2011
 27 respectively, while the shaded areas are one model standard deviation.

28



29
 30 **Figure S5** – pH diurnal profiles when not accounting for NVCs, for May (a), August (b),
 31 September (c) and November (d) at JST/RS/GT, July (e) and December (f) at YRK and for the
 32 SOAS campaign period (g). Blue and red lines are the CMAQ predicted pH for 2001 and 2011
 33 respectively, while the shaded areas are one model standard deviation. Green line represents the
 34 measurements and the shades area is standard error.

35



36

37 **Figure S6** – pH diurnal profiles with assimilated RH when NVCs are included in the calculations,
 38 for November at JST/RS/GT (a), the SOAS period (b) and July at YRK (c), and when NVCs are
 39 not included for November at JST/RS/GT (d), the SOAS period (e) and July at YRK (f). Blue and
 40 red lines are the CMAQ predicted pH for 2001 and 2011 respectively, while the shaded areas are
 41 one model standard deviation. Green line represents the measurements and the shades area is
 42 standard error.

43

44 **Organic acids and pH**

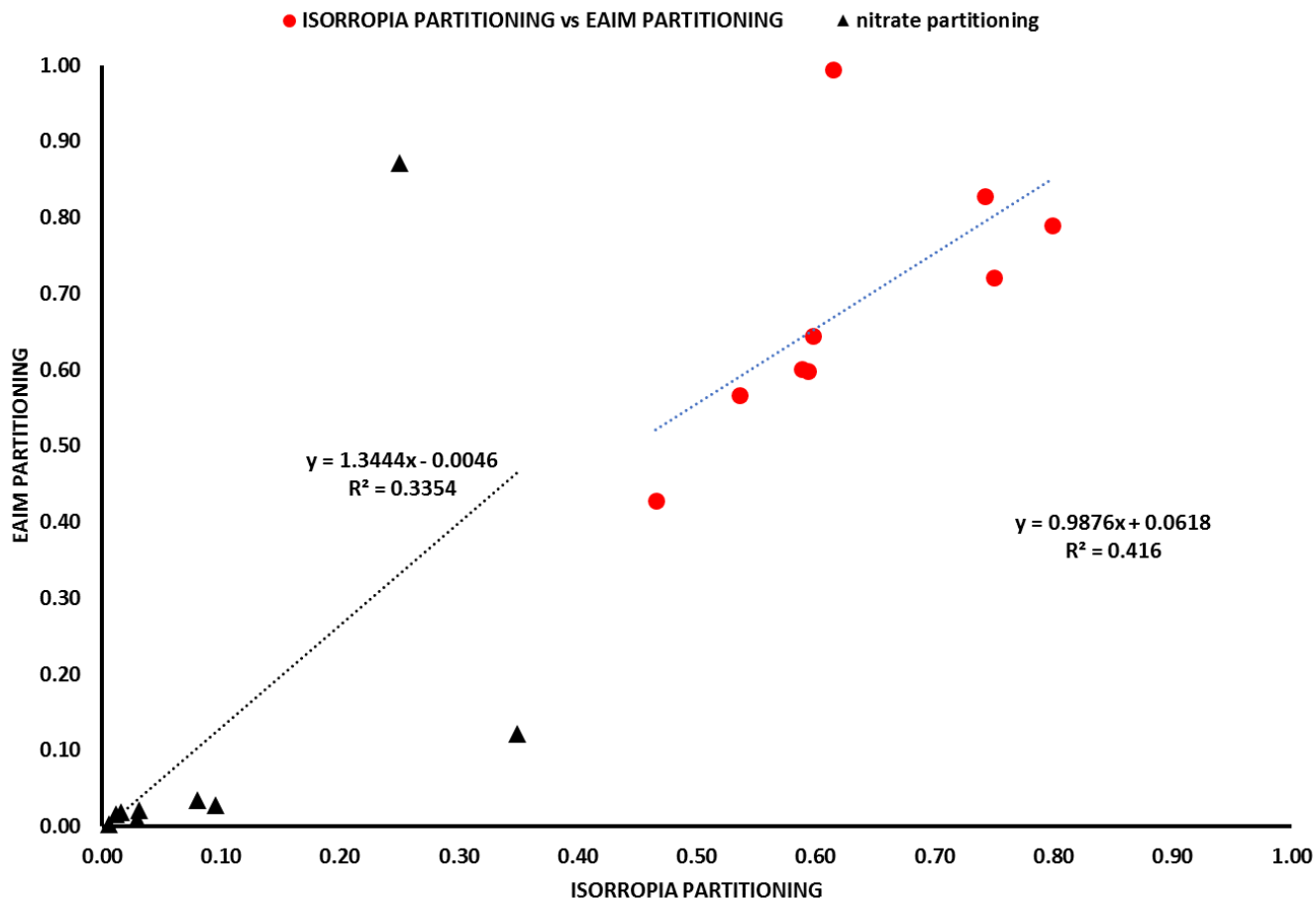
45 To determine the impact of organic compounds on acidity we tested a variety of scenarios
46 for our CMAQ results at the SEARCH sites, using the web-version of the Extended Aerosol
47 Inorganics Model (E-AIM) model (Wexler & Clegg 2002, Friese & Ebel 2010, Clegg et al. 1992)
48 (<http://www.aim.env.uea.ac.uk/aim/aim.php>). More specifically, we assumed that a set amount
49 (25 or 50% on a mole basis) of either oxalic, maleic, succinic or malonic acid already exists in the
50 aerosol phase but is not accounted for. Given the constant reductions in sulfate, we also tested the
51 potential of sulfate to be substituted by the same organics. To avoid the potential biases that NVCs
52 can incur on simulations, all runs were conducted without them. E-AIM was run using the
53 comprehensive Model IV configuration, in metastable mode. The baseline case that we used, was
54 the average composition, temperature and RH across all sites.

55 When comparing the total aerosol partitioning (particle to gas) for each SEARCH site
56 between ISORROPIA and E-AIM, they compare favorably, displaying an almost linear correlation
57 between the two (Fig. S7). For the low temperatures of December in Yorkville ($\bar{T} \leq 10^{\circ}\text{C}$) E-AIM
58 predicts a near complete absence of gas phase, in contrast to ISORROPIA, which is attributed to
59 the difference of how the activity coefficients are calculated between the two models (Wexler &
60 Clegg 2002, Friese & Ebel 2010, Clegg et al. 1992). Acidity between the two models differs, but
61 both predict sufficiently low values for pH for all sites (Table S2).

62 Initially, an amount of 25 or 50% of additional oxalic acid on a mole basis was added to
63 the baseline case, and then the pH was compared (Table S2). We find that for the cases presented
64 in this study, addition of organic compounds to the model did not have a significant impact on
65 acidity when compared to the baseline run, apart from the cases where RH was higher than 80%
66 and the mole fraction of organic acids in the aqueous phase is greater than 25%. pH remains rather
67 insensitive to the addition of oxalic acid for most cases, apart from the case that has the highest
68 RH=0.8, and subsequently the highest amount of liquid water. For all other cases, most of oxalic
69 acid partitions to the gas phase and its impact is negligible. Similarly, when other organic acids
70 are tested against the baseline, under the same conditions (maleic, succinic, malonic), they incur
71 a maximum 4% change on pH (Table S3).

72 For the substitution tests with oxalic acid, removal of sulfate from the system rapidly
73 decreases the amount of total water in the particulate phase (Fig. S8). This leads to the partitioning
74 of organics to the gas phase (Fig. S8), abating their impact on pH, since the relative composition
75 on a mole fraction basis remains largely the same.

76 The above analysis demonstrates that, for the cases presented in this paper, organics do not
77 have an appreciable impact on pH when only one liquid phase exists. Allowing more than one
78 liquid phase of different compositions to form, can still potentially impact pH (Pye et al. 2018).



79

80

81 **Figure S7** –Nitrate (black) and total (red) particle-to-gas partitioning predicted between E-AIM
 82 and ISORROPIA.

83

84

85

86

87

88

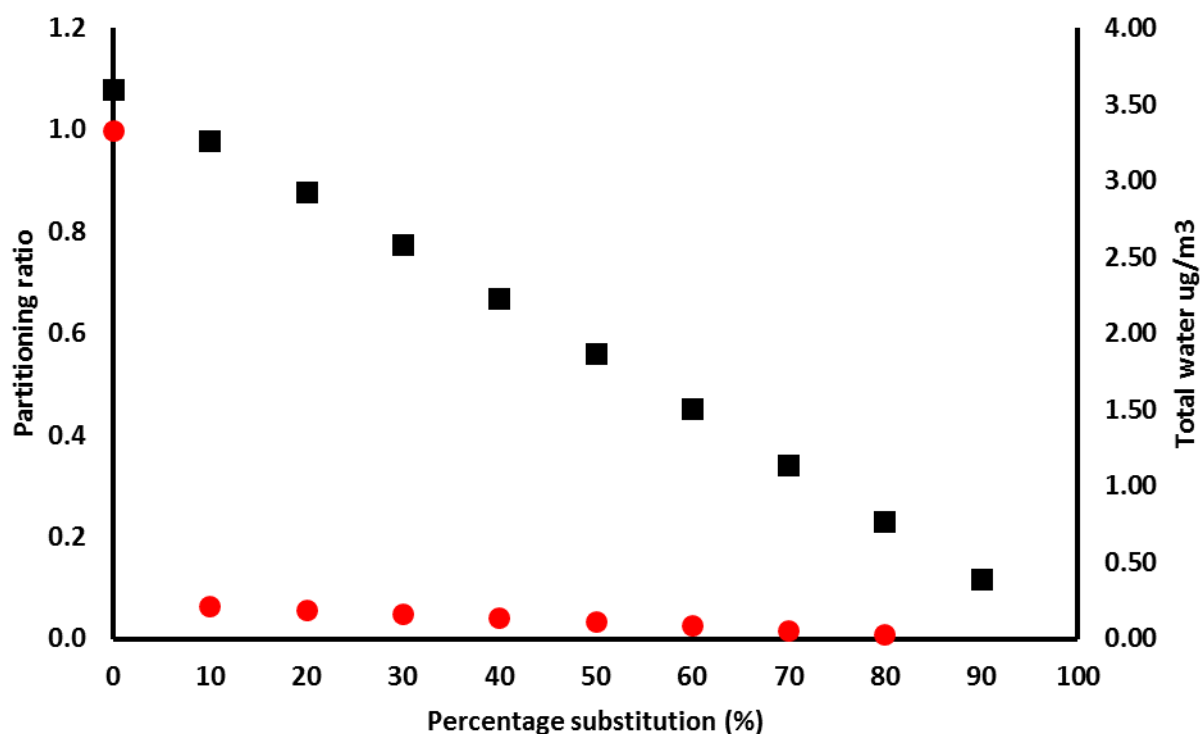
89

90

91 **Table S2** – ISORROPIA, E-AIM and E-AIM with an additional 25 and 50% oxalic acid
 92 predicted pH for all sites.

ISORROPIA PH	pH EAIM	pH 25% OXALIC	pH 50% OXALIC
-0.22	0.81	0.82	0.83
-0.30	0.92	0.92	0.91
0.55	1.31	1.32	1.25
-0.04	0.91	0.90	0.83
-0.01	0.55	0.55	0.55
0.07	0.34	0.34	0.34
0.14	0.53	0.53	0.52
-0.46	0.91	0.71	0.57
1.49	1.00	1.10	1.18

93
 94



95
 96 **Figure S8** –Comparison of predicted particle-to-gas partitioning of oxalic acid (red)
 97 water (black) between E-AIM and ISORROPIA as a function of sulfate substitution to oxalic
 98 acid.

99

100 **Table S3** – E-AIM predicted pH for the baseline case and for the cases with 25 and 50%
 101 addition of maleic, succinic or malonic acid.

Default pH EAIM	
0.809500489	
pH 25% MALEIC	pH 50% MALEIC
0.827689031	0.832387327
pH 25% SUCCINIC	pH 50% SUCCINIC
0.821886748	0.821886748
pH 25% MALONIC	pH 50% MALONIC
0.81276138	0.808548986

102

103

104 **The role of non-volatile cations in PM 2.5 pH**

105 To test whether the PM 2.5 pH bias can be attributed to the internally-mixed NVCs, we
 106 omit their presence and repeat the aerosol thermodynamic calculations (offline) for 2001 and 2011.
 107 The pH values of 2011 plotted against 2001 for each grid cell in the Eastern US study domain, for
 108 the winter (a) and summer (b) seasons are shown in Figure S10. On a seasonal basis, when NVCs
 109 are included in the thermodynamic calculations, for the winter the strongest biases are observed
 110 for gridcells that in 2001 had pH between -1 and 3, with differences becoming smaller with
 111 increasing pH. The largest differences during summer are localized for the gridcells that had pH
 112 values between -1 and 0.5 in 2001, while some gridcells from the Southern Lake Michigan and
 113 the coastal area of Massachusetts, New Hampshire, Maine and South Carolina exhibit very strong
 114 biases of 5 to 3 units. The proximity to marine aerosol and non-volatile Na is the underlying reason
 115 for this large change in aerosol pH.

116 With the removal of these NVCs and sea salt, there is remarkable agreement between the
 117 2001 and 2011 predicted PM_{2.5} pH, with only a small positive bias for the grid cells that in 2001
 118 had a pH of less than unity (Fig. S9). Although NVCs can sometimes comprise a significant

119 portion of PM_{2.5}, as it was the case for the SOAS campaign (Allen et al. 2015, Bondy et al. 2017),
 120 on average they should not be a major constituent of PM_{2.5} (Guo et al. 2015) over the Eastern
 121 US, which is indicative of a portion of coarse mode dust being distributed to the smaller sized
 122 aerosol in CMAQ, contrary to what has thus far been observed (Foroutan et al. 2017). While the
 123 dust emissions were the same between the 2001 and 2011 simulations, given the same meteorology
 124 for these years, and the fact that they were not scaled up/down in our model emissions, their impact
 125 became much larger in 2011 due to the reductions in sulfate. NVCs on average account for 0.39
 126 $\mu\text{g m}^{-3}$ of CMAQ PM_{2.5} both in 2011 and 2001 over the Eastern US, which a factor of 4 higher
 127 than the measured PM₁ NVCs during the WINTER campaign (Guo et al. 2016). There is no bias
 128 for the gridcells near coastal areas for this case, indicating that these areas were strongly affected
 129 by the abundance of sea salt aerosol in fine PM.

130 To verify this finding, we compared observations of NVCs from the Metrohm Monitor for
 131 AeRosol and Gases (MARGA) for the SOAS campaign, as well as the SEARCH and CSN sites,
 132 to CMAQ results. The average mass of modelled NVCs for these sites is 0.56 $\mu\text{g m}^{-3}$, when
 133 compared to 0.14 $\mu\text{g m}^{-3}$ for the SEARCH/CSN average, indicating a factor of 4 overestimation,
 134 mainly from crustal elements (K^+ , Ca^{+2} and Mg^{+2}), further corroborated by the findings of Pye et
 135 al. 2018, where the same comparison was carried out.

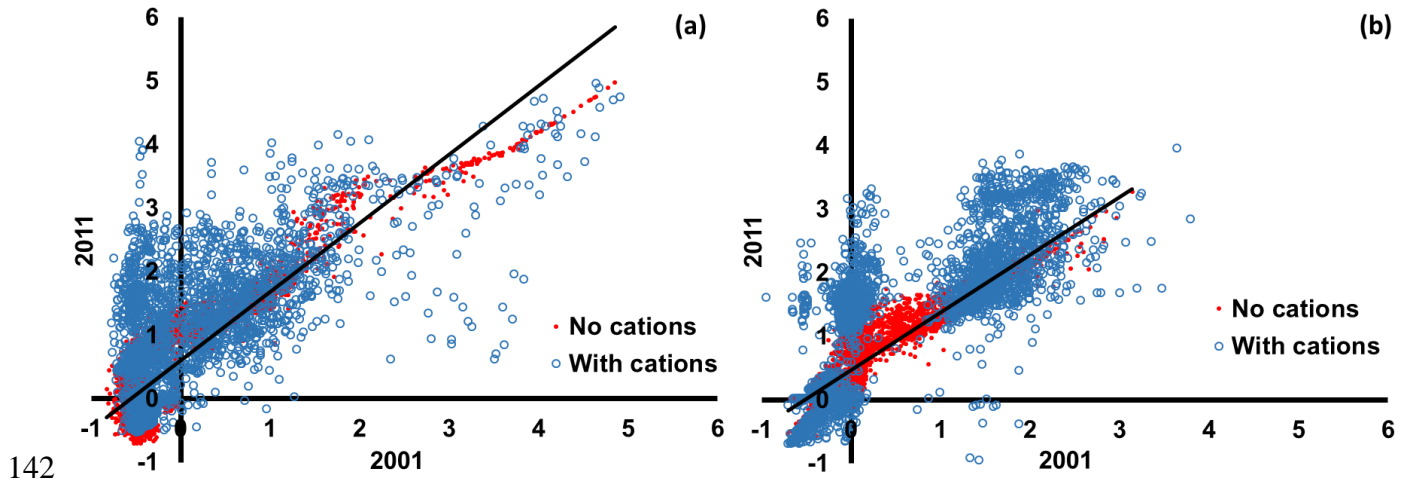
136
 137

138 **Table S4** – Comparison of NVCs ($\mu\text{g m}^{-3}$) between simulation results for the 3 SEARCH
 139 sites, and the measurements provided in Allen et al. 2015 and Pye et al. 2018

140

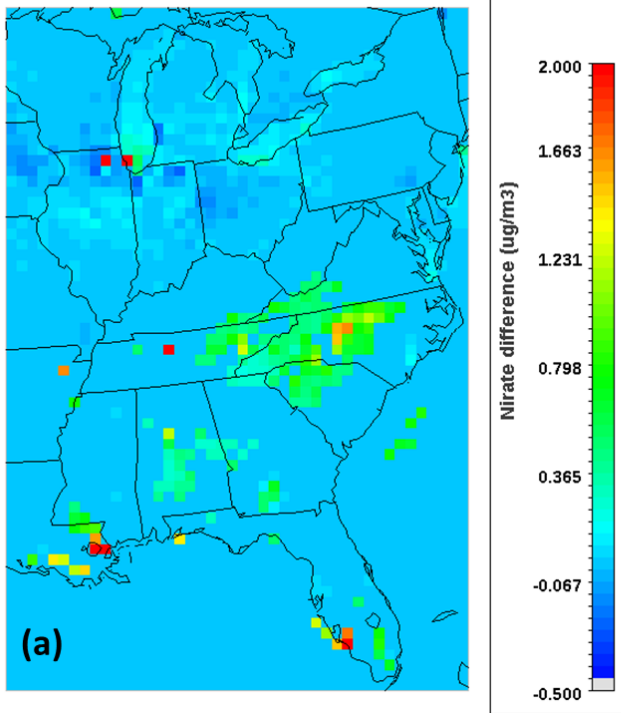
	Na	Mg	K	Ca	Total NVCs
JST AUG	0.024	0.033	0.135	0.462	0.653
JST MAY	0.039	0.040	0.146	0.473	0.697
JST NOV	0.053	0.049	0.192	0.533	0.826
JST SEP	0.029	0.038	0.155	0.450	0.671
YRK DEC	0.052	0.044	0.184	0.412	0.692
YRK JUL	0.014	0.010	0.063	0.098	0.185
CSN	0.050	0.000	0.060	0.030	0.140
SEARCH	0.050	-	0.060	0.030	0.140
SOAS	0.032	0.007	0.071	0.083	0.193
MARGA	0.074	0.010	0.045	0.047	0.175

141

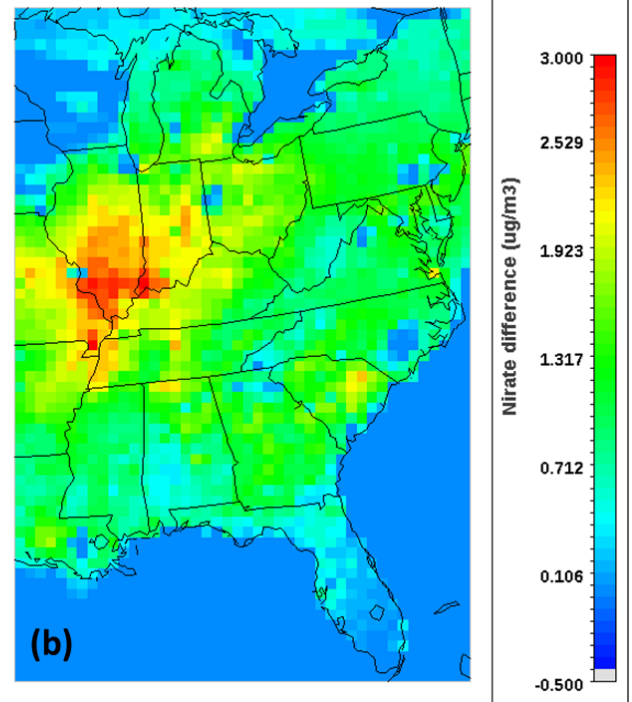


142
 143 **Figure S9** - Scatter plots of ISORROPIA predicted pH over the Eastern US study domain, for the
 144 winter (a) and summer (b), with and without NVCs.

Nitrate difference for July 2011



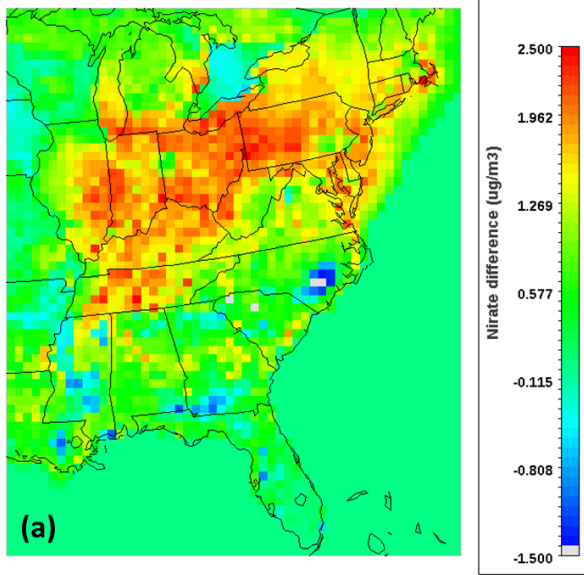
Nitrate difference for January 2011



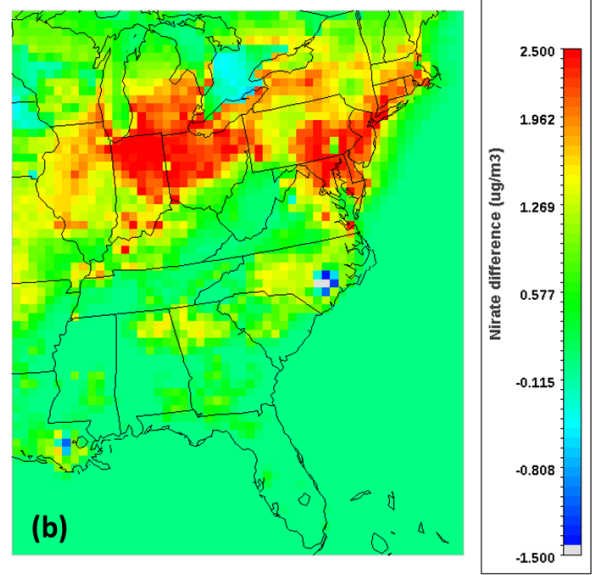
145
 146 **Figure S10** – Difference in nitrate over the Eastern US, between ISORROPIA predicted nitrate
 147 when NVCs are included in calculations, and when they are excluded, for July (a) and January (b)
 148 of 2011.

149

Difference of 2011 to 2001 NO3 with NVCs included



Difference of 2011 to 2001 NO3 without NVCs



150

151 **Figure S11** – Difference in predicted nitrate over the Eastern US between 2011 and 2001 when
152 NVCs are included in calculations (a), and when they are excluded (b).

153

154

155 **References**

- 156 Allen, H. M., D. C. Draper, B. R. Ayres, A. Ault, A. Bondy, S. Takahama, R. L. Modini, K.
157 Baumann, E. Edgerton, C. Knote, A. Laskin, B. Wang, and J. L. Fry (2015), Influence of crustal
158 dust and sea spray supermicron particle concentrations and acidity on inorganic NO₃⁻ aerosol
159 during the 2013 Southern Oxidant and Aerosol Study, *Atmospheric Chemistry and Physics*,
160 15(18), 10669-10685.
- 161 Bondy, A. L., B. Wang, A. Laskin, R. L. Craig, M. V. Nhliziyo, S. Bertman, K. A. Pratt, P. B.
162 Shepson, and A. P. Ault (2017), Inland Sea Spray Aerosol Transport and Incomplete Chloride
163 Depletion: Varying Degrees of Reactive Processing Observed during SOAS, *Environmental*
164 *Science & Technology*.
- 165 Clegg, S. L., Pitzer, K. S., and Brimblecombe, P., Thermodynamics of multicomponent, miscible,
166 ionic solutions. II. Mixtures including unsymmetrical electrolytes. *J. Phys. Chem.* 96, 9470-9479,
167 DOI: 10.1021/j100202a074, 1992
- 168 Foroutan, H., J. Young, S. Napelenok, L. Ran, K. W. Appel, R. C. Gilliam, and J. E. Pleim (2017),
169 Development and evaluation of a physics-based windblown dust emission scheme implemented
170 in the CMAQ modeling system, *J. Adv. Model. Earth Syst.*, 9, 585–608,
171 doi:10.1002/2016MS000823.
- 172 Friese, E. and Ebel, A., Temperature dependent thermodynamic model of the system H⁺ - NH₄⁺
173 - Na⁺ - SO₄²⁻ - NO₃⁻ - Cl⁻ - H₂O. *J. Phys. Chem. A*, 114, 11595-11631, DOI:
174 10.1021/jp101041j, 2010
- 175 Guo, H., Sullivan, A.P., Campuzano-Jost, P., Schroder, J.C., Lopez-Hilfiger, F.D., Dibb, J.E.,
176 Jimenez, J.L., Thornton, J.A, Brown, S.S., Nenes, A., and Weber, R.J. (2016) Fine particle pH and
177 the partitioning of nitric acid during winter in the northeastern United States, *J.Geoph.Res.*, 121,
178 doi:10.1002/2016JD025311
- 179 Guo, H., Xu, L., Bougiatioti, A., Cerully, K. M., Capps, S. L., Hite Jr., J. R., Carlton, A. G., Lee,
180 S.-H., Bergin, M. H., Ng, N. L., Nenes, A., and Weber, R. J.: Fine-particle water and pH in the

181 southeastern United States, *Atmos. Chem. Phys.*, 15, 5211-5228, doi:10.5194/acp-15-5211-2015,
182 2015.

183 Pye, H. O. T., Zuend, A., Fry, J. L., Isaacman-VanWertz, G., Capps, S. L., Appel, K. W., Foroutan,
184 H., Xu, L., Ng, N. L., and Goldstein, A. H.: Coupling of organic and inorganic aerosol systems
185 and the effect on gas–particle partitioning in the southeastern US, *Atmos. Chem. Phys.*, 18, 357-
186 370, <https://doi.org/10.5194/acp-18-357-2018>, 2018.

187 Wexler, A. S., and S. L. Clegg, Atmospheric aerosol models for systems including the ions H⁺,
188 NH₄⁺, Na⁺, SO₄²⁻, NO₃⁻, Cl⁻, Br⁻, and H₂O, *J. Geophys. Res.*, 107(D14), DOI:
189 10.1029/2001JD000451, 2002, <http://www.aim.env.uea.ac.uk/aim/aim.php>

190

191